ICWE14
June 21-26, 2015 | Porto Alegre - Brazil
14th INTERNATIONAL CONFERENCE ON WIND ENGINEERING

Torsional Instability of Single-Axis Solar Tracking Systems

Christian Rohr[1], Peter A. Bourke[1], David Banks[2]
[1]CPP Wind Engineering, St. Peters, NSW 2044, Australia
[2]CPP Wind Engineering, Fort Collins, Colorado, USA
email: crohr@cppwind.com, pbourke@cppwind.com, dbanks@cppwind.com

ABSTRACT: Anecdotal evidence suggests that single axis trackers have occasionally failed in the field due to significant, sudden excitation of their first mode of vibration. This mode features a gradual helical twisting that increases with distance from the torque motor. We have carried out section model simulations both with Computational Fluid Dynamics (CFD) and in a wind tunnel, to investigate the nature of the fluid-structure interaction. The instability is the result of vortices forming on, and then shedding from, the leading edge as it twists up and down. The sudden release of torque as the vortex is shed lead to torsional galloping, but only for trackers initially positioned roughly parallel to the ground. The wind tunnel simulations indicate that the instability is quite robust, with little success found in creating aerodynamic disruption of the vortices. The CFD work indicated a weak dependence on stiffness and damping. As a result, we recommend that isolated trackers and trackers on the edge of arrays not be positioned flat in high winds.

KEY WORDS: Torsional galloping, Solar tracking system, Aeroelastic Instability, Sectional model.

1 INTRODUCTION

Single axis trackers typically feature a long span (often 30 chords or more), the rotation of which is driven by a single central motor, or by a shaft connecting multiple rows to a larger motor. Running along the entire span at mid-chord is an axel, commonly called the torque tube. As their first mode of vibration, these systems typically have a helical twisting mode, with no deflection at the motor or shaft, and opposing rotations on either end. The torque tube is supported (and prevented from moving up or down) by piers or posts placed at regular intervals along the span. This means that it is much easier to twist the structure than to heave it up and down. This is a support structure unlike those commonly investigated for bridges.

It is common for the operators of solar tracking systems to have a policy of moving these systems into a "stow position" during high winds. This stow position is designed to minimize critical wind loads, and it is common for both single and dual axis trackers to adopt a flat stow position (parallel to the ground) to accomplish this. In this position, the trackers bear a resemblance to a bridge or a wing, so we investigated the potential for galloping or flutter using textbook instability theory.

This analysis indicated that classical flutter was not expected, because the trackers cannot heave up and down while twisting because their vertical motion is constrained at regular intervals along the span by the support posts, while the entire span from motor to tracker edge is able to twist in unison. Nor was galloping indicated by the equations, as for large aspect ratio rectangular cross-sections the stability condition is always satisfied.

Torsional galloping was not predicted either, at least for low tilt angles. Here is the equation for critical wind speed (U_{cr}) that is provided by (Blevins, 1990)

$$\frac{U_{cr}}{f_\theta C} = -\frac{8J_\theta(2\pi\zeta)}{\rho_a C^4} \Big/ \frac{\partial C_M}{\partial \alpha} \tag{1}$$

with a stability condition of

$$\frac{\partial C_M}{\partial \alpha} > 0 \tag{2}$$

where C_M is the torsional moment coefficient, ρ_a is the density of air, C is the chord length or width of the tracker, α is the angle of attack, J_θ is the polar mass moment of intertia about the pivot, ζ is the damping ratio, f_θ is the frequency of the twist motion. It is not worth providing the quasi-static moment coefficient derivatives we used from our wind tunnel testing of these systems,

because the equation is widely recognized not to be accurate for bluff sections shedding vortices. Here we quote directly from Blevins:

> "First, approximating the effect of torsional velocity of angle of attack with a single characteristic point is not viable for bluff sections… Second torsional flow induced vibrations of bluff sections are particularly sensitive to the vortices thrown off by the rotating section and quasi-steady theory cannot predict the associated unsteady vortex forces".

When we were first provided with evidence of an instability resembling torsional galloping happening to single axis trackers in the field, the tracker was twisting back and forth more than 20°, which we have also observed in our simulations. This suggests a third failing, because parts of these equations are derived from the incorrect assumption that angular changes are small (for example, to linearize the angle of attack and approximate the moment coefficient with a Taylor series expansion).

The form of these equations is helpful though. Equation (2) predicts torsional instability if the torsional moment coefficient drops with increasing twist angle (away from flat). The more sudden the loss of moment, the lower the critical velocity for the instability to occur becomes. Torsional galloping is sometimes called "stall flutter", as the sudden loss of lift due to the stalling of an airfoil can provide this big drop in torsional moment. But we can see no good way to get this derivative short of running an aeroelastic simulation.

Equation (1) indicates that we can expect the critical velocity to increase linearly with damping, and with the square root of stiffness, and indeed this is what we observed, see Results.

We are not aware of any published investigations of this instability in wind engineering. However, it has been investigated for the purpose of generating energy from the tides by Armandei and Fernandes (2012), who determined the critical water velocity for instability of two different paddle-spring systems. They also investigated the flutter derivatives (Scanlan and Tomko, 1971) related to this instability:

$$M = \rho U^2 C^2 \left(K \frac{C}{U} A_2^* \dot{\theta} + K^2 A_3^* \theta \right) \tag{3}$$

where $K = \omega C / U$ = reduced frequency, with ω as the frequency of the torsional motion. They concluded that A_2^* and A_3^* were both linear functions of approach flow speed above a certain speed.

It is interesting to note that the flutter derivatives imply a critical role for K, which is the ratio of leading edge speed to the speed of the oncoming flow. This ratio is very low for a single axis tracker, which typically twist at natural frequencies near 1 Hz, and have chords of around 2 m, so that the tip speed is only 1 m/s. We anticipate instability for wind speed more than 10 times this high, which raises the question as to whether this ratio is significant in this case.

2 EXPERIMENTAL PROCEDURE

2.1 Sectional Approach

This study is based purely on two-dimensional sectional models representing a given portion of a real, twisting single-axis tracker. The twisting under investigation is of helical shape, with no deflection at mid-span, and opposing rotations on either end. The stiffness of the sectional model was scaled to represent a contributing portion of span considered to actively be driving the motion of the entire system. This approach creates an envelope of potential responses inside which the response of the real, three-dimensional system is expected to lie.

2.2 CFD Model

The CFD model consisted of a transient 2D simulation with the same geometry as the wind tunnel test, but with the panel mounted approximately 1.2 metres above the ground. The domain was discretized into approximately 1 million quadrilateral cells, with significant refinement around the panel and wake region. For the purpose of observing the threshold at which instability occurs, the realizable k-epsilon turbulence model was deemed appropriate, Inlet turbulence intensity was 5%. Wall y+ values were generally maintained between 30 and 300, although this was not always the case after instability when the panel was at peak angular velocities. Inlet speeds and turbulence intensities were constant.

A wide range of wind speeds, start angles, stiffness values, and damping values were simulated. Stiffness and damping were modelled outside of the CFD. The CFD simulation was coupled to a physics solver which used the equation of motion:

$$J_\theta \ddot{\theta} + 2 J_\theta \zeta \omega_\theta \dot{\theta} + k_\theta \theta = M = ½ \rho U^2 C^2 C_M \tag{4}$$

2.3 Wind Tunnel Model

A stiff sectional model of a typical single-axis solar panel tracking system was placed horizontally in CPP's atmospheric boundary layer wind tunnel located in Sydney, Australia. A variable stiffness torsional spring was attached to the axis of rotation, and angular displacement was measured with a laser sensor mounted next to the panel. The panel was mounted outside the boundary layer of the wind tunnel, and end effects on the panel were negated by adding end plates to either end of the panel.

See Figure 1. The system was tested primarily at 0 yaw. The wind speed in the tunnel was slowly increased until instability was observed. Turbulence intensity at panel height was roughly 3%.

Some aerodynamic treatments were added to the leading edge, though details cannot be provided as these are proprietary studies.

Figure 1. Wind tunnel section model

3 RESULTS

3.1 CFD Model

An image sequence showing the fluid structure interaction as the tracker goes unstable is shown in Figure 2. The process involves a cyclical increase in angle of attack which leads to vortex shedding.

Wind loading will cause an initial upward deflection of the leading edge (LE) of the panel (0.3 sec), the size of which depends on stiffness. A tight re-attachment is evident, leading to suction on the upper side for the quarter chord nearest the leading edge. As the incidence of the panel increases, the separation bubble increases in size, until eventually it is no longer attached (0.55 sec). There is now a mild suction across the entire top surface, so the LE begins to twist back down. It springs past the 0° (flat) position, and a vortex forms near the LE on the underside, creating significant suction on the LE quarter chord (0.77 sec). As it twists down, the separation bubble gets bigger (lowering the moment), the resistance goes up, and eventually the panel stops twisting (0.9sec). Once again the reattachment is lost. The panel springs back upward, past 0°, and a tight vortex forms on the top surface by the LE (1.05 sec). The vortex grows until it sheds (1.2 seconds), at which point lift and moment are lost, and the process repeats, each time with a higher angular deflection.

The simulation in Figure 2 does not include the ground. Adding the ground did not significantly change this flow pattern. It did create a secondary instability when the leading edge is tilted down into the wind. In this situation, only the lower edge sheds a vortex, and the motion is typically restricted to twisting below the plane of the axis. The twist angle can be large enough to damage a tracker (+/-20°).

The cycle of twisting and moment for a similar simulation is plotted in Figure 3. The loss of moment becomes increasingly rapid as the displacement increases and the vortex shedding becomes more pronounced. Trailing edge vortices are also shed in between each cycle, but are of smaller magnitude. These account for the smaller spikes in the moment coefficient curves.

The instability is characterized by vortex shedding which eventually happens in lock-step with twisting at the natural frequency of the structure. These are also characteristics of vortex lock-in, and as a result we have at times referred to this process as vortex lock-in. Classic vortex lock-in has a range of wind speeds where the instability occurs, whereas this instability clearly has a critical velocity above which it will always go unstable, and is qualitatively well-described by the torsional galloping equations presented in the introduction.

Simulations were run at different wind speeds and the time series of displacements were examined to determine if the tracker was unstable or not. Sample results are shown in Figure 4. Note that the decay rate is not always adequate. Case DP 71 clearly decays to a stable displacement, while the amplitude of the DP 72 curves grows throughout the simulation. DP 62, on the other hand, reaches something of a steady state. But it is twisting at +/-70°, which is more than enough to break the tracker, so this is considered unstable as well. Simulations also resulted in marginally unstable behaviours (Figure 5), which were helpful in pinpointing the critical wind speed.

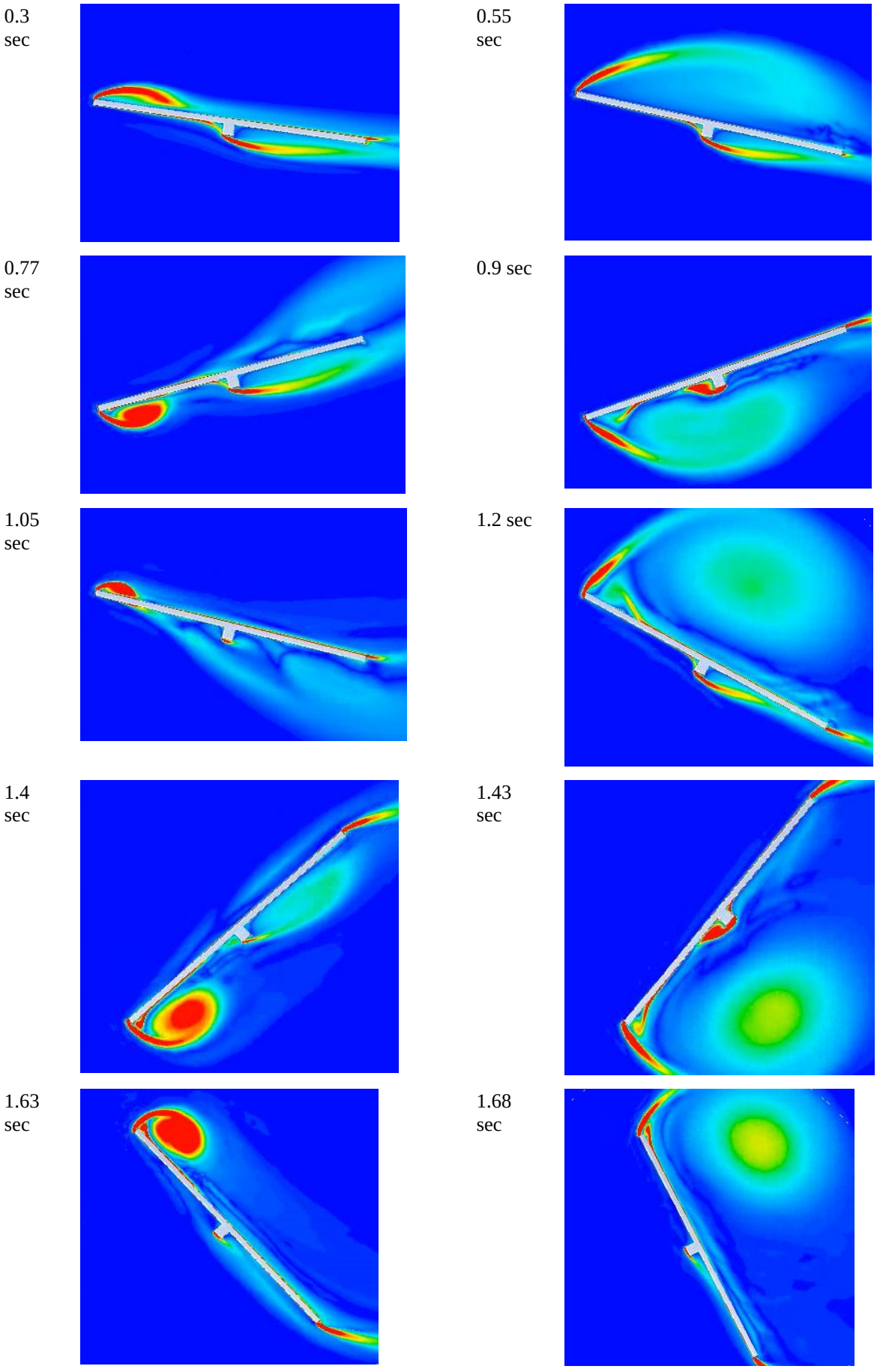

Figure 2. Contours of vorticity. On the left, the vortex is strong, on the right, there is no longer reattachment.

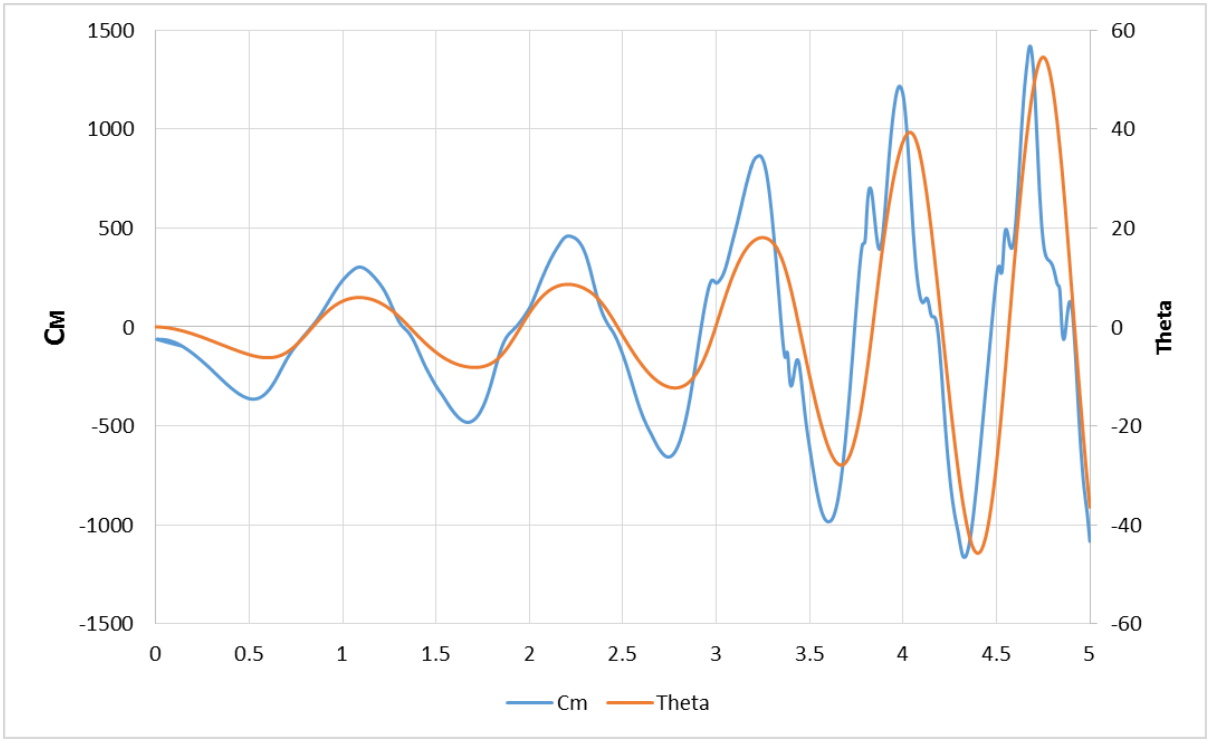

Figure 3. Cycles of moment coefficient and rotation.
Note: Moment coefficient values illustrate pattern only, they are normalized to arbitrary small unit dimensions and speeds.

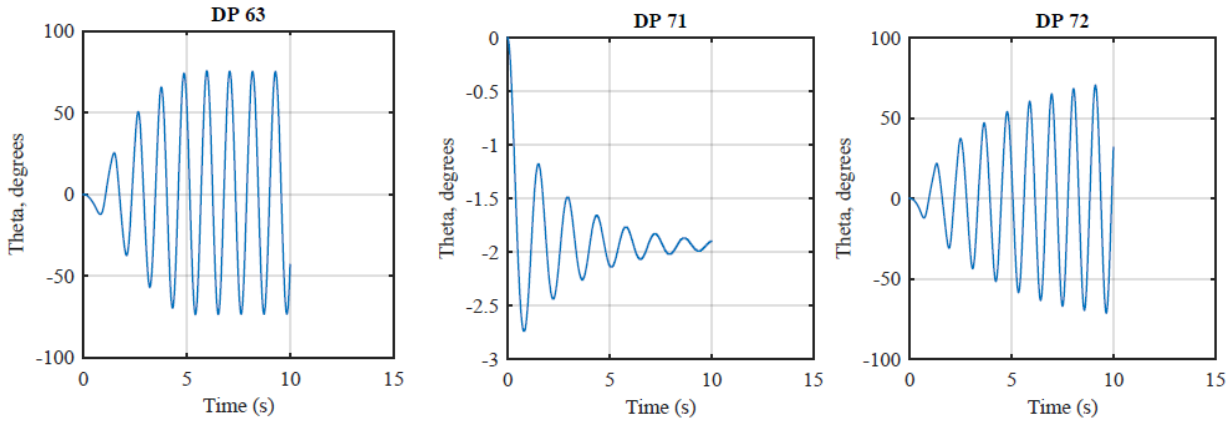

Figure 4. Time series of rotation for difference simulations

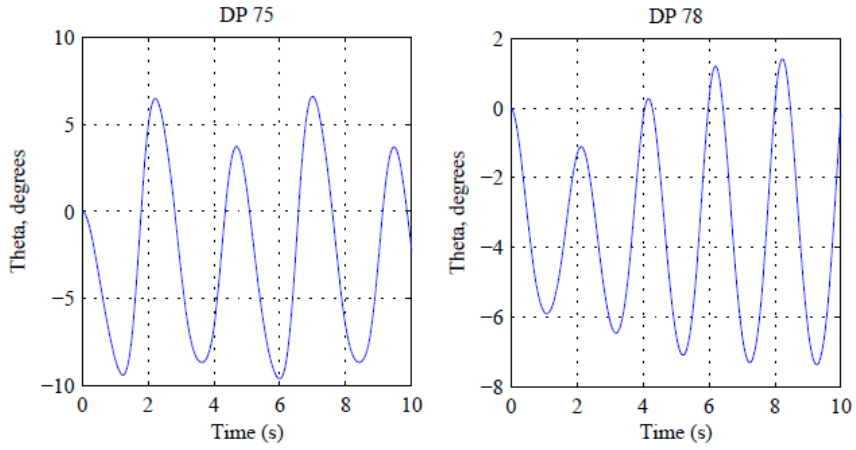

Figure 5. Time series of rotation for simulations near U_{cr}

3.2 Wind Tunnel Model

The instability was readily reproduced in the wind tunnel. The instability is very robust, and features a hysteresis, where once the wind speed rises above U_{cr}, it must drop considerably below U_{cr} before the tracker becomes stable again. Several aerodynamics treatments were added to the leading edge to disrupt the vortex formation, as this has been shown to prevent vortex formation on low-rise building roofs (Banks, 2001). While these devices were able to delay the onset of instability (modestly increasing U_{cr}), once the instability was initiated, the motion reached greater twist angles more quickly than when U_{cr} was first exceeded without the treatments. We believe that this indicates that once galloping starts, the edge treatment is no longer helping at all, and the twisting displacements are similar to what would be observed at that speed without any edge treatment. This is hazardous to the test rig.

The wind tunnel model was used to validate the CFD model, and it showed good agreement (Figure 6). Error bars are shown on the CFD data points to indicate the distance to the next data point – wind speed increments of 5 and 10 m/s were used, so that the exact location of the instability lies within the bars. The agreement was reasonable, though the wind tunnel experiments provided a higher critical wind speed.

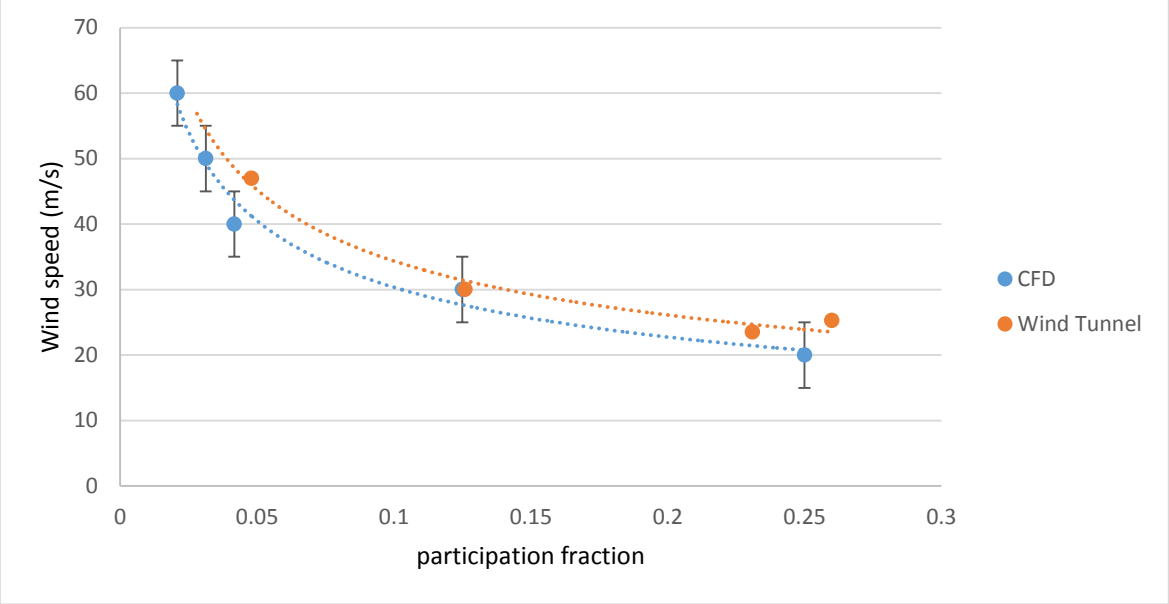

Figure 6. Critical wind speed comparison, wind tunnel vs. CFD.

4 DICUSSION

4.1 Interpreting the results

Figure 6 plots U_{cr} against "participation fraction" on the x-axis. Participation fraction is a rough estimate of the portion of the tracker that is shedding vortices. Since the interior of the tracker (nearest the motor or drive shaft) twists very little, we would expect that only the outer portion of the tracker is moving enough to be actively participating in vortex shedding. We expect there will be positive feedback, so that if the outer 15% starts shedding, the next 5% will soon have enough displacement to join in, so that the outer 20% is now taking part.

The smaller the participation fraction, the more stiffness is present in the rest of the non-participating tracker to resist the motion, so stiffness is the inverse of participation fraction.

The critical wind speed depends significantly on the participation fraction, which need to be determined through a three dimensional simulation or full scale testing. However, our results indicate that most trackers which are not sheltered from the wind can expect issues with torsional galloping at wind speeds below 40 m/s if stowed flat. Given the rapid onset of lock-in and the hysteresis, we believe that U_{cr} determined from the steady CFD inlet speeds should be considered as gust speeds (at panel height) of a duration of 3 seconds.

4.2 Fixing the problem

The simplest way to avoid this instability is to stow the trackers at an angle. However, high tilt angles introduce greater static loads as well as increased dynamic excitation due to buffeting in the array interior, which will need to be considered in the design.

The CFD simulations indicated that the instability was not very sensitive to the moderate levels of damping (3%-15%) typical of such systems. We believe this is because there is only a small portion of the cycle during which the aerodynamics are not acting to force the tracker to twist in its first mode.

CONCLUSIONS

Single axis trackers are susceptible to torsional galloping, in which a vortex forms above the leading edge of the tracker, creating significant moment about the center chord. As the tracker twists upward, the size of the flow separation increases, and the zone of significant uplift crosses the midpoint of the chord. Rather than slowly losing torque, though, the loss of moment becomes sudden and severe as the vortex is shed from the tracker. The tracker then bounces back past the flat position, and now has its leading edge twisted downward into the wind. A vortex then forms on the underside of the leading edge, and the process repeats itself.

Our investigation has shown this mechanism to be extremely robust and of concern for many existing tracker designs. It is possible to excite twisting in the first mode shape with only a fraction of the full span participating in the vortex shedding and with significant amplitudes be achieved in only a few cycles.

The instability can be avoided at typical non-hurricane design wind speeds through a combination of stow policy (variable tracker position through the array), damping, and stiffness.

ACKNOWLEDGEMENTS

We would like to thank NEXTracker for supporting this research and preemptively developing a solution. Visit cppwind.com for more information.

REFERENCES

M. Armandei and A. C. Fernandes, "Stability Analysis Of A Yawing Flat Plate Into The Water Current", *Proceedings of the ASME 2012 31st International Conference on Ocean, Offshore and Arctic Engineering*, July 1-6, 2012, Rio de Janeiro, Brazil, 2012.

D. Banks , P. P. Sarkar , F. Wu and R. N. Meroney, "A Device to Mitigate Vortex Induced Rooftop Suction", *Proceedings of the Americas Conference on Wind Engineering*, Baltimore, 2001.

R. D. Blevins, *Flow-Induced Vibration*, 2nd edition, New York, Van Nostrand Reinhold, 1990.

Y. Nakamura and T. Matsukawa, "Vortex Excitation of Rectangular Cylinders with a Long Side Normal to the Flow", *Journal of Fluid Mechanics*, 180, 171-191, 1987.

R. H. Scanlan, J. J. Tomko, "Airfoil and bridge deck flutter derivatives". *ASCE Journal of the Engineering Mechanics Division*; 97, 1717–1737, 1971